

A Study of Four Southern RR Lyrae Stars Based on MASTER, TESS, and ASAS-SN Data

T. V. Migal^{1,2}, A. N. Tarasenkov¹, V. M. Lipunov^{3,1}, P. V. Balanutsa^{1,4}, A. S. Kuznetsov¹, M. M. Shilova¹,
C. Francile^{5,6}, F. Podesta^{5,6}

¹ Sternberg Astronomical Institute, Moscow State University, Universitetskij pr. 13, Moscow 119992, Russia

² Moscow Institute of Physics and Technology, Institutsky per. 9, Dolgoprudny 141700, Russia

³ Lomonosov Moscow State University, GSP-1, Leninskie Gory, Moscow, 119991, Russia

⁴ National Research Center Kurchatov Institute, 123098, Moscow, Russia

⁵ Observatorio Astronomico Felix Aguilar (OAFa), Avda Benavides 8175, Rivadavia, El Leonsito, San Juan 5400, Argentina

⁶ Facultad de Ciencias Exactas Fisicas y Naturales, San Juan National University, Casilla de Correo 49, San Juan 5400, Argentina

We present our photometric analysis of four RR Lyrae variables detected by the MASTER robotic net. Variability of these stars was detected by automatic routines for detecting astrophysical transients based on frame subtraction algorithms. To clarify the variability type and period, we used the TESS and ASAS-SN data. As a result, the VSX classification and period were corrected for one of the stars, SSS J195436.8-522301, and periods were refined for three others: Gaia DR3 6012658518794440064, SSS J134829.5-225501, and V2247 Sgr.

1 Introduction

One of the main scientific goals of the MASTER Robotic Net is to search for new astrophysical transients and variable objects (Lipunov et al. 2010). The search for transients is performed using a special automatic detection system, which can use different operating modes to search for different types of transients (Kornilov et al. 2012; Gorbovskoy et al. 2013; Lipunov et al. 2019). The main search algorithm is to compare two frames taken within a short interval of time with an archival reference frame. This method allows us to find flares and outbursts of various astrophysical nature: GRBs, outbursts of cataclysmic variables, flares of UV Ceti stars, etc. (Lipunov et al. 2022, Lipunov et al. 2024), as well as to identify fading and variable objects (Lipunov et al. 2016). However, to search for supernovae and weakly variable objects, the frame subtraction method is usually used. It demonstrates high efficiency under non-uniform background illumination and, in particular, made it possible to detect a kilonova (an optical counterpart of the GW170817 event, Abbott et al. 2017ab; Lipunov et al. 2017).

While exploring transient candidates, variable stars are often detected by the auto-detection system as transient candidates, but usually not enough attention is paid to their detailed study. Using data from the TESS space mission (Ricker et al. 2015) allows us to solve this problem, since the TESS data archive permits to obtain continuous light curves for almost any variable star. This paper describes the discovery and study of four RR Lyrae variable stars identified by the MASTER network auto-detection system, which were identified with the known variables, based on TESS data. All four variables

were detected on frames obtained by the MASTER-OAFA telescope in Argentina. Since the periods and variability types published in the VSX database (Watson et al. 2006) for the objects under study were obtained by automatic systems, they are not correct for some stars. Light curves, obtained from TESS data for each of these stars, reveal their true types and pulsation periods. Since TESS data have a fairly high photometric accuracy, they make classification and period determination possible. However, the light curve duration is 27 days of continuous monitoring, and there may be biases in the time calculation between sectors (Volkova & Volkov 2025), so we used ASAS-SN (Shappee et al. 2014, Kochanek et al. 2017) data where possible to accurately determine the period.

2 Investigation of RR Lyrae variables

To extract TESS photometry, we used a *Python* script (Tarasenkov 2024) based on the *Lightkurve* library (Lightkurve Collaboration et al. 2018). The photometric apertures for the object and background were set to maximize the flux from the object and minimize the effects of background illumination and contamination from field stars. Next, outliers and trends were removed using a polynomial fit. The result were purified light curves, then subjected to periodogram analysis.

To study periodicities in the TESS data, the Lomb–Scargle periodogram (VanderPlas 2018) implemented in the *Astropy* package (Astropy Collaboration et al. 2013) was used. For accurate determination of the period based on ASAS-SN data, the Deeming (1975) method implemented in the WinEfk program¹ was used.

2.1 SSS J195436.8-522301

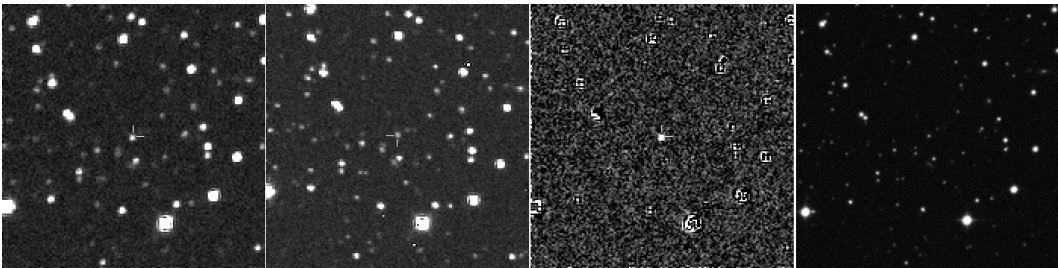


Figure 1.

MASTER-OAFA $6' \times 6'$ cutout frames of SSS J195436.8-522301. From left to right: detection frame, comparison frame, difference frame, and POSS2 Red archival plate cutout.

The variable star SSS J195436.8-522301 (ASASSN-V J195436.84-522303.3) (J2000 coordinates: RA = $19^{\text{h}}54^{\text{m}}36^{\text{s}}.78$, Decl = $-52^{\circ}23'03''.2$) was identified as a periodic variable by Catalina Siding Spring Survey (Drake et al. 2017) and ASAS-SN survey (Jayasinghe et al 2018, 2020). In the latter survey, the object is designated as a rotating variable (ROT type in VSX) with a period of $1^{\text{d}}0046$.

Variability of SSS J195436.8-522301 was detected on frames obtained by the MASTER-OAFA robotic telescope at 2025-08-04 02:02:43 UT with limiting magnitude of $19^{\text{m}}1$ in the unfiltered band. The comparison archive frame was taken at 2025-06-24 05:18:21 UT with limiting magnitude of $20^{\text{m}}3$ in unfiltered band. Variability of SSS J195436.8-522301 is clearly visible in the difference frame (see Fig. 1).

¹<http://www.vgoranskij.net/software/>

Table 1: **Individual periods of SSS J195436.8-522301 from TESS data**

	Sector 13	Sector 27	Sector 67	Sector 94
Period, days	0.503	0.502	0.501	0.502
Error, days	0.004	0.004	0.004	0.005

SSS J195436.8-522301 was observed by the TESS space mission in Sectors 13, 27, 67 and 94. Periodogram analysis of TESS data reveals that the object is misclassified in the Drake et al. (2017) catalog. A period of $0^d502 \pm 0^d005$, twice shorter than that determined by ground-based means, is clearly revealed. The error was estimated as the width of the peak of the power spectrum at the half of its height. Period calculations for individual sectors are presented in Table 1. The light curves, folded with these periods, show a clearly asymmetric shape with a short ascending branch and a smoother decline. The geometry of the curve is stable throughout the entire TESS observation period, which is completely uncharacteristic for most spotted stars. The periodograms with highlighted best frequency and folded light curves of SSS J195436.8-522301 are shown in Fig. 2. The light curves obtained from data from later sectors have more data points and stronger scattering due to shorter exposure times used. Since TESS has a very large pixel size ($\sim 21''$) and the target is quite faint (about 17^m5 in the V band), contamination from neighboring stars cannot be completely subtracted even using special algorithms. Therefore, an exact determination of the amplitude is impossible.

For SSS J195436.8-522301, no high-quality observations of ASAS-SN are available, so it is impossible to derive the period with a high accuracy.

The period, the characteristic asymmetric light curve, as well as the presence of a small bump before the minimum, allow us to conclude that SSS J195436.8-522301 is an RR Lyrae star pulsating in the fundamental mode (RRAB type). The overall shape of the light curve does not show any obvious changes in amplitude, so we argue that the Blazhko effect is either absent or has a small amplitude that cannot be detected without further observations.

2.2 Gaia DR3 6012658518794440064

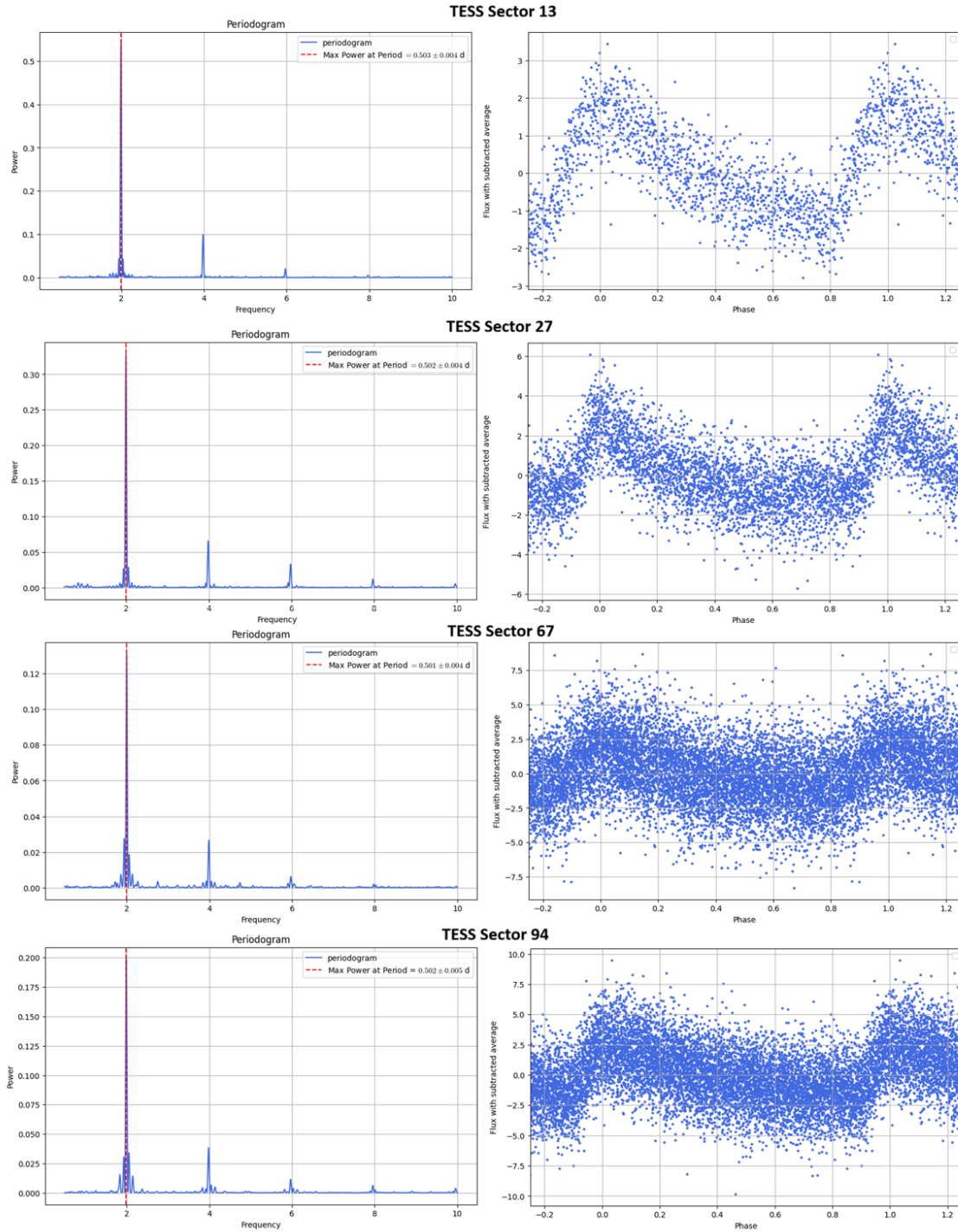
Variability of Gaia DR3 6012658518794440064 was detected on frames obtained by the MASTER-OAFA robotic telescope at 2025-08-04 01:52:38 UT with the limiting magnitude of 17^m68 in unfiltered band. The comparison archive frame was taken at 2025-07-28 00:22:06 UT with the limiting magnitude of 19^m1 in unfiltered band. Variability of Gaia DR3 6012658518794440064 is clearly visible in the difference frame (see Fig. 3).

The variable Gaia DR3 6012658518794440064 (J2000 coordinates: $15^h29^m20^s16$, $-37^\circ28'20''.7$) is identified as an RRAB variable in the Gaia variability catalog (Gaia collaboration et al. 2023). TESS observed Gaia DR3 6012658518794440064 in Sector 65. The periodogram analysis reveals the period of $0^d624 \pm 0^d007$, which is consistent with the period given in the VSX and Gaia variability catalog.

The light curve of Gaia DR3 6012658518794440064, like that of the previous variable, has an asymmetric shape with a rapid ($\sim 20\%$ of the period) rise to the maximum and a slower decline, characteristic of RR Lyrae stars. The periodogram and folded light curve are presented in Fig. 4. We were unable to identify the presence of Blazhko effect for this star. Thus, we confirm the classification of Gaia DR3 6012658518794440064, presented in the VSX, as an RR Lyrae star pulsating in the fundamental mode (RRAB type).

To improve the period, we computed it using the WinEfk program from ASAS-SN

SSS J195436.8-522301

**Figure 2.**

Periodograms (left panels) and folded light curves (right panels) for SSS J195436.8-522301 based on TESS data.

data. The Deeming method was used, with the error calculated from the set of periods that gave the best-quality light curve. The resulting period is $0^{\text{d}}.6244117 \pm 0^{\text{d}}.0000001$, and the full light elements are $C = 2459358.6127 + 0^{\text{d}}.6244117 \times E$. The ASAS-SN light curve, folded with these elements, and the periodogram for these data are shown in Fig. 5.

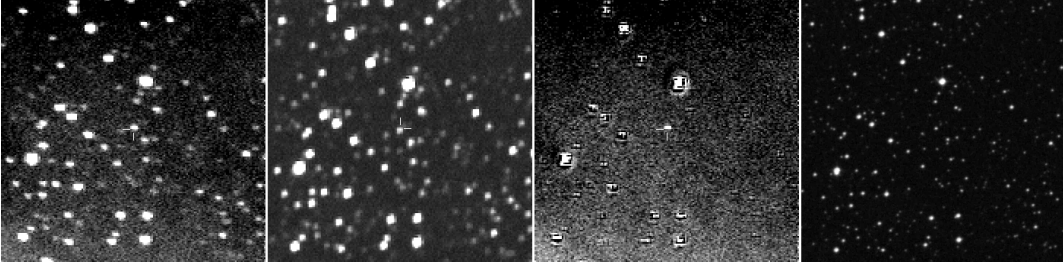


Figure 3.

MASTER-OAFA $6' \times 6'$ cutout frames of Gaia DR3 6012658518794440064. From left to right: detection frame, comparison frame, difference frame, and POSS2 Red archival plate cutout.

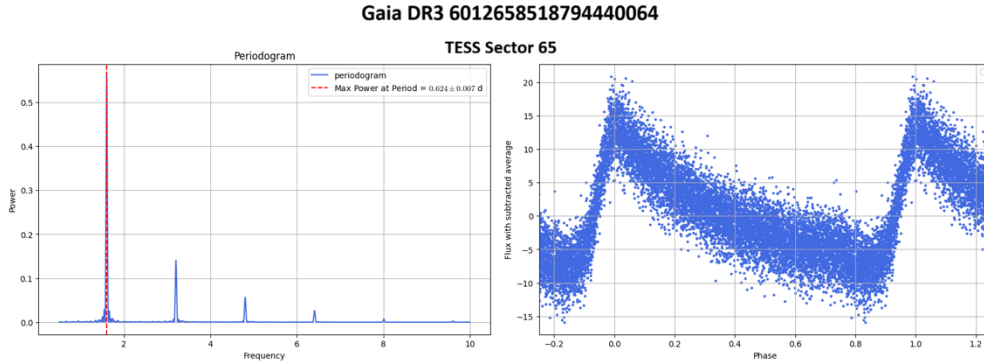


Figure 4.

Periodogram (left panel) and folded light curve (right panel) for Gaia DR3 6012658518794440064 based on TESS data.

2.3 SSS J134829.5–225501

Variability of SSS J134829.5–225501 was detected on frames obtained by the MASTER-OAFA robotic telescope at 2025-08-05 01:31:37 UT with limiting magnitude of $17^{\text{m}}.83$ in unfiltered band. The comparison archive frame was taken at 2025-04-05 05:04:49 UT with limiting magnitude of $20^{\text{m}}.65$ in unfiltered band. Variability of SSS J134829.5–225501 is clearly visible in the difference frame (see Fig. 6).

The variable SSS J134829.5–225501 (ASASSN-V J134829.48–225500.7) (J2000 coordinates: $13^{\text{h}}48^{\text{m}}29^{\text{s}}.53$, $-22^{\circ}55'01''.2$) was identified as a periodic variable by the Catalina Siding Spring Survey (Drake et al. 2017) and the ASAS-SN survey (Jayasinghe et al. 2018, 2020).

TESS observed SSS J134829.5–225501 in Sectors 37, 64, and 91 in 2021, 2023 and 2025. Table 2 presents the results of period determination for these sectors by the Lomb–Scargle method.

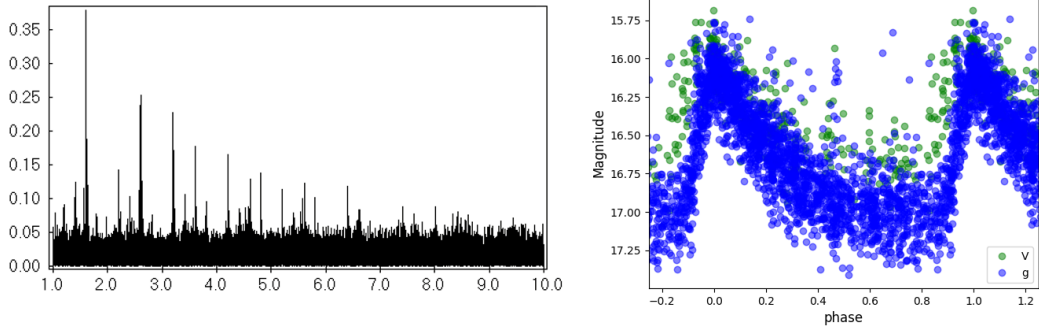


Figure 5.

Periodogram (left panel) and folded light curve (right panel) for Gaia DR3 6012658518794440064 based on ASAS-SN data.

Table 2: Individual periods of SSS J134829.5-225501 from TESS data

	Sector 37	Sector 64	Sector 91
Period, days	0.450	0.450	0.450
Error, days	0.003	0.004	0.003

As the result, the pulsation period of SSS J134829.5–225501 can be estimated as $0^{\text{d}}.450 \pm 0^{\text{d}}.004$. It is in a good agreement with the period reported in VSX.

The period of SSS J134829.5–225501 does not show noticeable changes over the TESS observation time. Other harmonics were also not reliably detected. The light curve corresponds to the RRC type: it has an approximately symmetric sinusoidal shape, with a small bump at the phase ~ 0.75 , which is observed for many RRC stars. Although this object is listed as RRD in the VSX database, we cannot confirm this classification because of no reliably detected multiperiodicity. It is possible that SSS J134829.5–225501 experienced a mode switch from double-mode to single-mode pulsations. A similar effect was observed for some RR Lyrae stars (Soszyński et al. 2014, Khruslov et al. 2017). Therefore, we classify SSS J134829.5–225501 as an RRC star at the time of TESS observations.

To improve the period, we determined it using the WinEfk program from ASAS-SN data. The Deeming method was used, with the error calculated from a set of periods that gave the best shape of the light curve. The resulting period is $0^{\text{d}}.4496661 \pm 0^{\text{d}}.0000002$, the full light elements being $C = 2458708.5232 + 0^{\text{d}}.4496661 \times E$. The ASAS-SN light curve, folded with these elements, and the periodogram for these data are shown in Fig. 8.

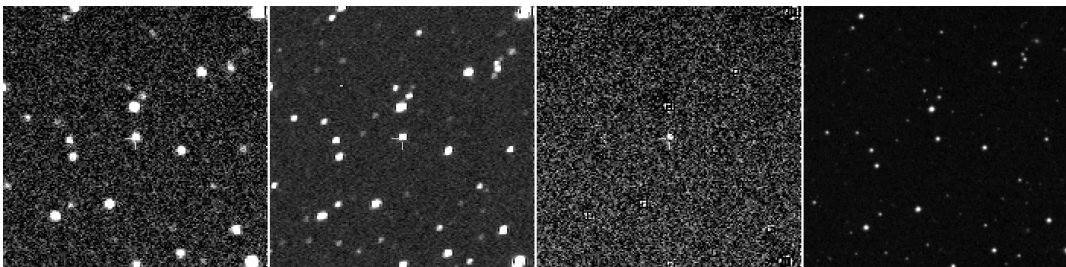


Figure 6.

MASTER-OAFA $6' \times 6'$ cutout frames of SSS J134829.5-225501. From left to right: detection frame, comparison frame, difference frame, and POSS2 Red archival plate cutout.

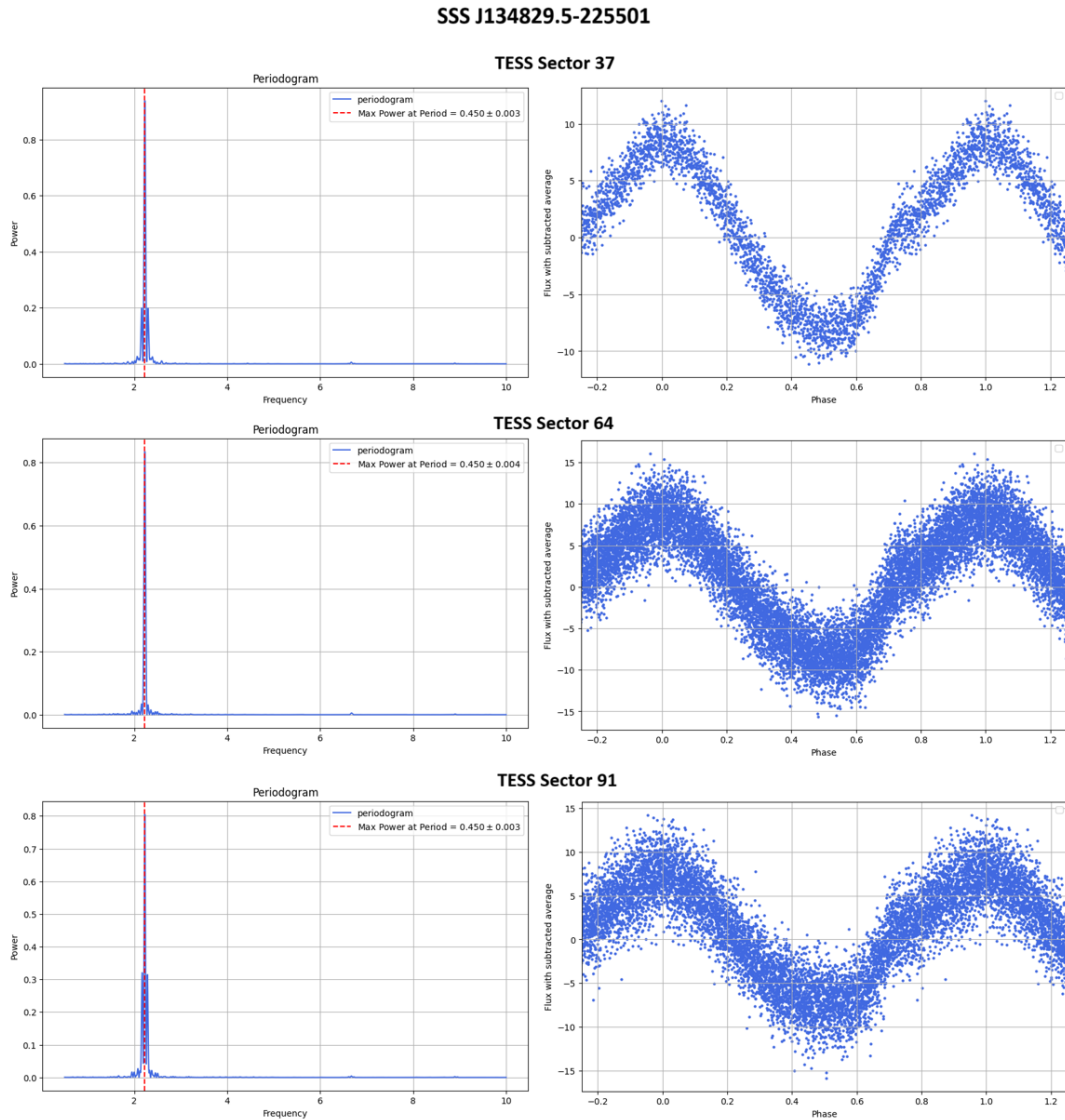


Figure 7.

Periodograms (left panels) and folded light curves (right panels) for SSS J134829.5-225501 based on TESS data.

2.4 V2247 Sgr

The variable star V2247 Sgr was identified by MASTER autodetection system on frames obtained by the MASTER-OAFA robotic telescope at 2025-08-01 03:11:51 UT with limiting magnitude of 19^m33 in unfiltered band. The comparison archive frame was taken at 2025-07-02 04:28:27 UT with limiting magnitude 19^m88 in unfiltered band. Variability of V2247 Sgr is clearly visible in the difference frame (see Fig. 9).

Variability of V2247 Sgr was first discovered by Hoffmeister (1963). The star enters the GCVS (Samus' et al. 2017) as an RR variable. V2247 Sgr (J2000 coordinates: $20^h13^m04^s.12$, $-38^\circ09'37''.4$) was also identified as an RR Lyrae variable by Catalina Survey (Torrealba et al. 2015) and Gaia (Clementini et al. 2019, 2023). The star was also observed by WISE in the mid-infrared (Gavrilchenko et al. 2014). TESS observed this

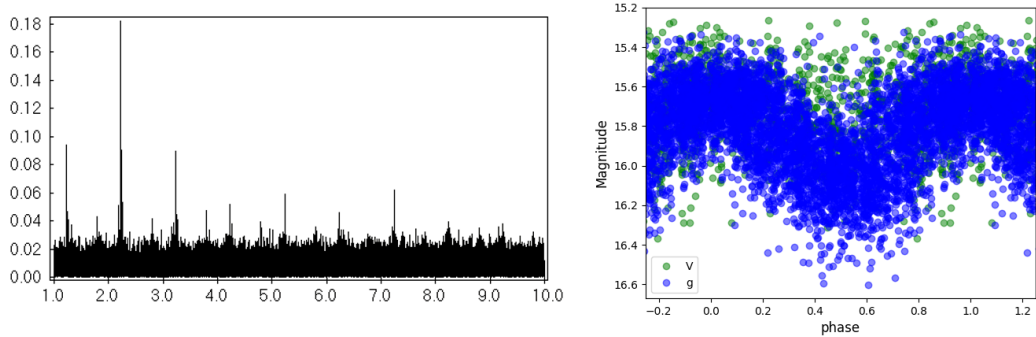


Figure 8.

Periodogram (left panel) and folded light curve (right panel) for SSS J134829.5-225501 based on ASAS-SN data.

star in 3 sectors in 2020, 2023 and 2025, but only Sector 67 data (observed in 2023) allowed us to obtain a light curve, while in other sectors, the target was inaccessible due to instrumental limitations.

The Lomb–Scargle periodogram gives the period of $0^{\text{d}}445 \pm 0^{\text{d}}003$, which agrees well with that in VSX.

The folded light curve shows asymmetric shape characteristic of RRAB stars. The duration of the ascending branch is approximately 10% of the period, while the descending branch is much longer. The light curve is shown in Fig. 10. We therefore confirm the RRAB classification of V2247 Sgr given in VSX.

To improve the period, we determined it using the WinEfk code from ASAS-SN data. The Deeming method was used, with the error calculated from the set of periods giving the best light curve. The resulting period is $0^{\text{d}}4451676 \pm 0^{\text{d}}0000001$, the full light elements being $C = 2460835.6596 + 0^{\text{d}}4451676 \times E$. The ASAS-SN light curve folded with these elements and the periodogram for these data are shown in Fig. 11.

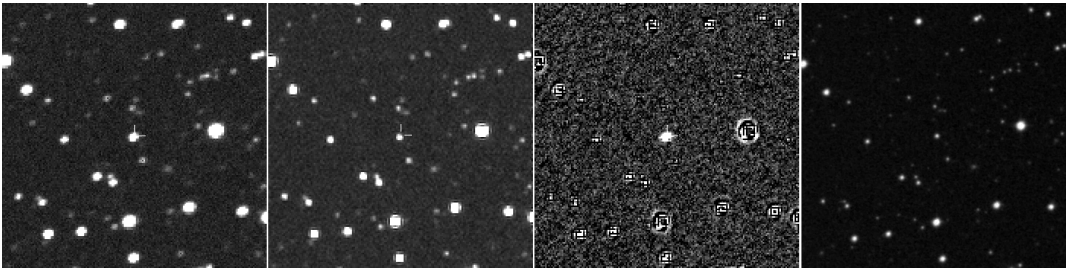


Figure 9.

MASTER-OAFA $6' \times 6'$ cutout frames of V2247 Sgr. From left to right: detection frame, comparison frame, difference frame, and POSS2 Red archival plate cutout.

3 Discussion

This work shows that the automatic processing tools of the MASTER network, developed for detecting astrophysical transients (Lipunov et al. 2019), can be used to detect variable

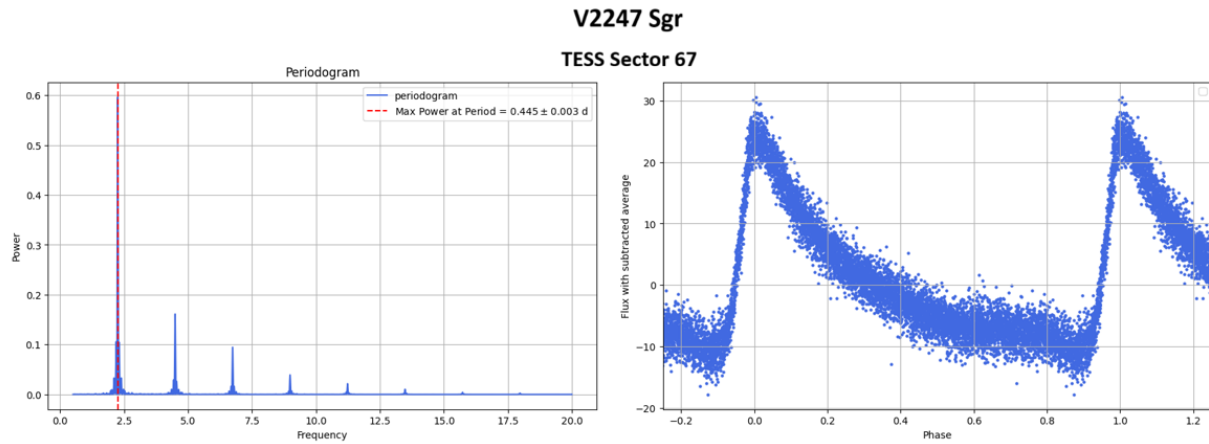


Figure 10. Periodogram (left panel) and folded light curve (right panel) for V2247 Sgr based on TESS data.

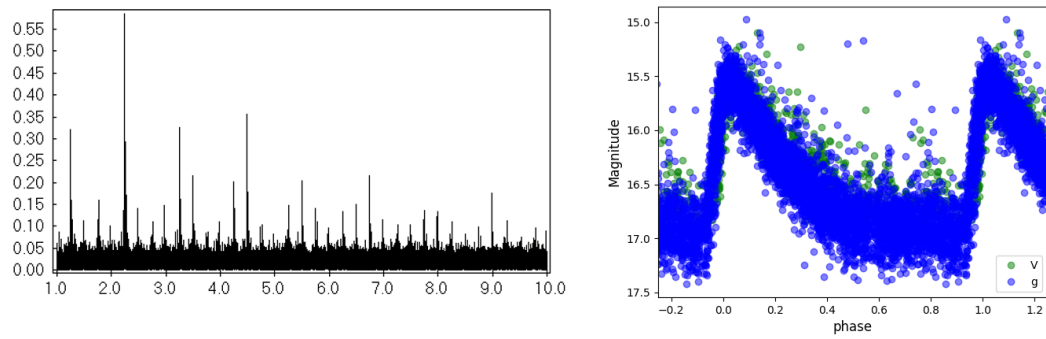


Figure 11. Periodogram (left panel) and folded light curve (right panel) for V2247 Sgr based on ASAS-SN data.

Table 3: Stars studied in the present paper

Star	α, δ J2000.0	Type	P
SSS J195436.8–522301	$19^{\text{h}}54^{\text{m}}36^{\text{s}}.78, -52^{\circ}23'03''.2$	RRAB	$0^{\text{d}}.502$ $\pm 0^{\text{d}}.005$
Gaia DR3 6012658518794440064	$15^{\text{h}}29^{\text{m}}20^{\text{s}}.16, -37^{\circ}28'20''.7$	RRAB	$0^{\text{d}}.6244117$ $\pm 0^{\text{d}}.0000001$
SSS J134829.5–225501	$13^{\text{h}}48^{\text{m}}29^{\text{s}}.53, -22^{\circ}55'01''.2$	RRC	$0^{\text{d}}.4496661$ $\pm 0^{\text{d}}.0000002$
V2247 Sgr	$20^{\text{h}}13^{\text{m}}04^{\text{s}}.12, -38^{\circ}09'37''.4$	RRAB	$0^{\text{d}}.4451676$ $\pm 0^{\text{d}}.0000001$

stars, including those with a relatively small variability amplitude, such as pulsating variables. Since the MASTER network has an extensive archive of images obtained over 20 years of operation (Tarasenkov et al. 2024a), this stimulates a systematic search for variable stars of selected types and studies of their properties (Tarasenkov et al. 2026).

However, this approach is not optimal for RR Lyrae stars because the accuracy and duty cycle of MASTER measurements do not provide sufficient capabilities to resolve subtle variations in the light curves, such as the Blazhko effect. Therefore, for such variables, it is necessary to combine different data sources for the most complete study, as suggested in a number of studies (Li et al. 2022; Juraev et al. 2025a; Tarasenkov et al. 2024b).

The crucial part of such studies is using data from the TESS mission, which provides high-quality data for studying pulsating stars. TESS supplies dense, high-precision light curves that allow us to determine periods with high accuracy, including the case of multiperiodicity (Juraev et al. 2025b), to track the Blazhko effect (Wilhelm et al. 2023), and even to estimate physical parameters of RR Lyraes and other pulsating stars (Kumar et al. 2025).

4 Conclusions

As a result of verification of optical transient candidates proposed by the MASTER network’s automatic detection system using the frame subtraction method, we identified four variable stars. We performed an analysis of TESS photometry for all these stars, which allowed us to classify them as RR Lyrae variables, determine their subtype and exact period. The results are presented in Table 4.

This result shows that the frame-subtraction transient detection system used on the MASTER network telescopes can detect objects whose variability amplitude is quite small by the standards of astrophysical transients ($1\text{--}2^{\text{m}}$). Moreover, the use of TESS data for analyzing the shape of the light curve and ASAS-SN data for calculating the exact period allows us to achieve a high quality of classification that is inaccessible to mass automatic identification systems.

Acknowledgements. A.Tarasenkov acknowledges the support of the Foundation for the Development of Theoretical Physics and Mathematics BASIS (project 25-2-1-39-1). The authors express their sincere gratitude to the Gravity Frontiers Foundation for supporting the team and this research. MASTER database research is carried out using the equipment of the shared research facilities of HPC computing resources at Lomonosov MSU (Voevodin et al. 2019). The study was conducted under the state

assignment of Lomonosov MSU. The authors would like to thank Dr. V. P. Goranskij for the opportunity to use the WinEfk code and Prof. N. N. Samus for useful comments that helped to improve the article.

References:

- Abbott, B. P., Abbott, R., Abbott, T. D., et al. 2017a, *Nature*, **551**, No. 7678, 85
- Abbott, B. P., Abbott, R., Abbott, T. D., et al. 2017b, *Astrophys. J. Letters*, **848**, No. 2, article id. L12
- Astropy Collaboration, Robitaille, T. P., Tollerud, E. J., Greenfield, P, et al. 2013, *Astron. & Astrophys.*, **558**, article id. A33
- Clementini, G., Ripepi, V., Garofalo, A., et al. 2023, *Astron. & Astrophys.*, **674**, article id. A18
- Clementini, G., Ripepi, V., Molinaro, R., et al. 2019, *Astron. & Astrophys.*, **622**, article id. A60
- Deeming, T. J. 1975, *Astrophys. & Space Sci.*, **36**, No. 1, 137
- Drake, A. J., Djorgovski, S. G., Catelan, M., et al. 2017, *Monthly Notices Roy. Astron. Soc.*, **469**, No. 3, 3688
- Gaia Collaboration, Vallenari, A., Brown, A. G. A., Prusti, T., et al. 2023, *Astron. & Astrophys.*, **674**, article id. A1
- Gavrilchenko, T., Klein, C. R., Bloom, J. S., & Richards, J. W. 2014, *Monthly Notices Roy. Astron. Soc.*, **441**, No. 1, 715
- Gorbovs koy, E. S., Lipunov, V. M., Kornilov, V. G., et al. 2013, *Astron. Reports*, **57**, No. 4, 233
- Hoffmeister, C. 1963, *Veröff. Sternwarte Sonneberg*, **6**, 1
- Jayasinghe, T., Kochanek, C. S., Stanek, K. Z., et al. 2018, *Monthly Notices Roy. Astron. Soc.*, **477**, No. 3, 3145
- Jayasinghe, T., Stanek, K. Z., Kochanek, C. S., et al. 2020, *Monthly Notices Roy. Astron. Soc.*, **491**, No. 1, 13
- Juraev, B. Sh., Burkhonov, O. A., Ehgamberdiev, Sh. A., et al. 2025a, *Astron. & Astrophys. Transactions*, **35**, No. 3, 275
- Juraev, B., Burkhonov, O., Ehgamberdiev, S. A., et al. 2025b, *Perem. Zvezdy / Variable Stars*, **45**, No. 13, 115
- Khruslov, A. V., Kusakin, A. V., & Reva, I. V. 2017, *Acta Astronomica*, **67**, No. 4, 317
- Kochanek, C. S., Shappee, B. J., Stanek, K. Z., et al. 2017, *Publ. Astron. Soc. Pacific*, **129**, No. 980, 104502
- Kornilov, V. G., Lipunov, V. M., Gorbovs koy, E. S., et al. 2012, *Experimental Astronomy*, **33**, No. 1, 173
- Kumar, N., Singh, H. P., Malkov, O., et al. 2025, *Universe*, **11**, No. 7, id. 207
- Li, L.-J., Qian, S.-B., & Zhu, L.-Y. 2022, *Monthly Notices Roy. Astron. Soc.*, **510**, No. 4, 6050
- Lightkurve Collaboration, Cardoso, J. V. M., Hedges, C., et al. 2018, *Astrophysics Source Code Library*, record ascl:1812.013
- Lipunov, V. M., Balanutsa, P. V., Pavlenko, E. P., et al. 2024, *Astron. Reports*, **68**, No. 12, 1364
- Lipunov, V., Gorbovs koy, E., Afanasiev, V., et al. 2016, *Astron. & Astrophys.*, **588**, article id. A90
- Lipunov, V. M., Gorbovs koy, E., Kornilov, V. G., et al. 2017, *Astrophys. J. Letters*, **850**, No. 1, article id. L1

- Lipunov, V., Kornilov, V., Gorbovskey, E., et al. 2010, *Advances in Astronomy*, article id. 349171
- Lipunov, V. M., Kornilov, V. G., Topolev, V. V., et al. 2022, *Astron. Letters* **48**, No 11, 623
- Lipunov, V. M., Vladimirov, V. V., Gorbovskey, E. S., et al. 2019, *Astron. Reports* **63**, No. 4, 293
- Ricker, G. R., Winn, J. N., Vanderspek, R., et al. 2015, *Journal of Astronomical Telescopes, Instruments, and Systems*, **1**, article id. 014003
- Samus', N. N., Kazarovets, E. V., Durlevich, O. V., et al. 2017, *Astron. Reports*, **61**, No. 1, 80
- Shappee, B. J., Prieto, J. L., Grupe, D., et al. 2014, *Astrophys. J.*, **788**, No. 1, article id. 48
- Soszyński, I., Udalski, A., Szymański, M. K., et al. 2014, *Acta Astronomica*, **64**, No. 3, 177
- Tarasenkov, A. N. 2024, *INASAN Science Reports*, **9**, No. 3, 89
- Tarasenkov, A. N., Lipunov, V. M., Antipov, G. A., et al. 2024a, *Lobachevskii J. Math.*, **45**, 3188
- Tarasenkov, A. N., Lipunov, V. M., Kuznetsov, A. S., et al. 2026, *Astrophys. & Space Sci.*, **371**, id. 22
- Tarasenkov, A., Zubareva, A. M., Maslennikova, N., et al. 2024b, *Perem. Zvezdy Prilozh. / Variable Stars Suppl.*, **24**, No. 1, 1
- Torrealba, G., Catelan, M., Drake, A. J., et al. 2015, *Monthly Notices Roy. Astron. Soc.*, **446**, No. 3, 2251
- VanderPlas, J. T. 2018, *Astrophys. J. Suppl. Ser.*, **236**, No. 1, article id. 16
- Voevodin, V. V., Antonov, A. S., Nikitenko, D. A., et al. 2019 *Supercomput. Front. Innov.*, **6**, No. 2, 4
- Volkova, A. S. & Volkov, I. M. 2025, *Astron. Reports*. **69**, No. 11, 1169
- Watson, C. L., Henden, A. A., & Price, A. 2006, in *The Society for Astronomical Sciences 25th Annual Symposium on Telescope Science*, Big Bear, CA, May 23-25, 2006
- Wilhelm, R., Carrell, K., Means, H. H., et al. 2023, *Astron. J.*, **165**, No. 5, id. 194